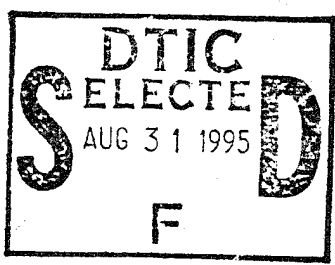# NATIONAL ADVISORY COMMITTEE
FOR AERONAUTICS

———

REPORT 952

DIRECT METHOD OF DESIGN AND STRESS ANALYSIS OF ROTATING DISKS WITH TEMPERATURE GRADIENT

By S. S. MANSON

1950

SEP 1 1950

AERONAUTIC SYMBOLS

1. FUNDAMENTAL AND DERIVED UNITS

	Symbol	Metric		English	
		Unit	Abbreviation	Unit	Abbreviation
Length_____	l	meter_____	m	foot (or mile)_____	ft (or mi)
Time_____	t	second_____	s	second (or hour)_____	sec (or hr)
Force_____	F	weight of 1 kilogram_____	kg	weight of 1 pound_____	lb
Power_____	P	horsepower (metric)_____	_____	horsepower_____	hp
Speed_____	V	{kilometers per hour_____	kph	miles per hour_____	mph
		{meters per second_____	mps	feet per second_____	fps

2. GENERAL SYMBOLS

W Weight $=mg$

g Standard acceleration of gravity $=9.80665$ m/s² or 32.1740 ft/sec²

m Mass $=\dfrac{W}{g}$

I Moment of inertia $=mk^2$. (Indicate axis of radius of gyration k by proper subscript.)

μ Coefficient of viscosity

ν Kinematic viscosity

ρ Density (mass per unit volume)

Standard density of dry air, 0.12497 kg-m⁻⁴-s² at 15° C and 760 mm; or 0.002378 lb-ft⁻⁴ sec²

Specific weight of "standard" air, 1.2255 kg/m³ or 0.07651 lb/cu ft

3. AERODYNAMIC SYMBOLS

S Area

S_w Area of wing

G Gap

b Span

c Chord

A Aspect ratio, $\dfrac{b^2}{S}$

V True air speed

q Dynamic pressure, $\dfrac{1}{2}\rho V^2$

L Lift, absolute coefficient $C_L=\dfrac{L}{qS}$

D Drag, absolute coefficient $C_D=\dfrac{D}{qS}$

D_0 Profile drag, absolute coefficient $C_{D_0}=\dfrac{D_0}{qS}$

D_i Induced drag, absolute coefficient $C_{D_i}=\dfrac{D_i}{qS}$

D_p Parasite drag, absolute coefficient $C_{D_p}=\dfrac{D_p}{qS}$

C Cross-wind force, absolute coefficient $C_C=\dfrac{C}{qS}$

i_w Angle of setting of wings (relative to thrust line)

i_t Angle of stabilizer setting (relative to thrust line)

Q Resultant moment

Ω Resultant angular velocity

R Reynolds number, $\rho\dfrac{Vl}{\mu}$ where l is a linear dimension (e.g., for an airfoil of 1.0 ft chord, 100 mph, standard pressure at 15° C, the corresponding Reynolds number is 935,400; or for an airfoil of 1.0 m chord, 100 mps, the corresponding Reynolds number is 6,865,000)

α Angle of attack

ϵ Angle of downwash

α_0 Angle of attack, infinite aspect ratio

α_i Angle of attack, induced

α_a Angle of attack, absolute (measured from zero-lift position)

γ Flight-path angle

REPORT 952

DIRECT METHOD OF DESIGN AND STRESS ANALYSIS OF ROTATING DISKS WITH TEMPERATURE GRADIENT

By S. S. MANSON

Lewis Flight Propulsion Laboratory
Cleveland, Ohio

I

Accesion For		
NTIS CRA&I	☑	
DTIC TAB	☐	
Unannounced	☐	
Justification		
By		
Distribution /		
Availability Codes		
Dist	Avail and / or Special	
A-1		

REPORT 952

DIRECT METHOD OF DESIGN AND STRESS ANALYSIS OF ROTATING DISKS WITH TEMPERATURE GRADIENT

By S. S. MANSON

SUMMARY

A method is presented for the determination of the contour of disks, typified by those of aircraft gas turbines, to incorporate arbitrary elastic-stress distributions resulting from either centrifugal or combined centrifugal and thermal effects. The specified stresses may be radial, tangential, or any combination of the two. For example, the equivalent stress may be specified at each radius inasmuch as this stress is generally used as the criterion of the occurrence of plastic flow. Use is made of the finite-difference approach in solving the stress equations, the amount of computation necessary in the evolution of a design being greatly reduced by the judicious selection of point stations and by the aid of a design chart. Use of the charts and of a preselected schedule of point stations is also applied to the direct problem of finding the elastic- and plastic-stress distribution in disks of a given design, thereby effecting a great reduction in the amount of calculation compared with previously published methods. Illustrative examples are presented to show computational procedures in the determination of a new design and in analyzing an existing design for elastic stress and for stresses resulting from plastic flow.

INTRODUCTION

The important role of the disk in the gas turbine has directed much attention to the analysis of stresses in rotating disks with temperature gradient. Early in the development of stress analysis of steam turbines, Stodola (reference 1) presented the basic equation for stresses in such disks, as well as a limited approach toward the solution. More recently, in connection with the development of the gas turbine for aircraft propulsion, the problem of determining thermal stresses resulting from temperature gradient has been actively investigated. Several methods have been developed (references 2 to 5) that can be used to calculate the stresses in a given disk due to differential expansion and to variation in physical properties of various parts of the disk operating at different temperatures. Thus, for disks already designed, it is readily possible to determine with a high degree of accuracy the centrifugal and thermal stresses resulting from a given speed and temperature distribution.

Little attention has, however, been directed towards the problem of designing the profile of a disk, which, when operated at a given speed and temperature distribution, will incorporate a given total-stress system—centrifugal plus thermal. A direct method of design for prescribed total-stress systems was developed at the NACA Lewis laboratory during 1948. Although the design method can readily be extended to include plastic flow, in the interest of simplicity only elastic stresses are considered.

The specified stresses may be either radial or tangential values, as is common in engineering practice, or the specification may refer to any combination of these stresses. For example, specification of the equivalent stress at each radius may be desired inasmuch as this stress is frequently used as a criterion of the occurrence of plastic flow. The method is based on the finite-difference equations derived in reference 3 and makes use of several simple design charts, presented herein, that facilitate the calculations. An illustration is presented for tracing the actual steps that may be followed in evolving a design.

A simplified method of analyzing an existing disk for centrifugal and thermal stress is also described. The method is especially useful in checking the stresses in a disk designed for prescribed stress distributions, particularly if minor deviations from the design profile are introduced for practical reasons, or if creep or plastic flow, not considered during the design stage, are likely to occur. Applications to arbitrary disks are equally valid. Essentially, the method is an adaptation of the finite-difference approach of references 3 and 4, the principal modifications lying in the use of a preselected distribution of point stations and the addition of several alinement charts to facilitate the computations.

Although the methods presented are of special advantage in calculations involving thermal stresses, they are suitable for disks subjected solely to centrifugal effects. Simple equations may be obtained both for design or for stress analysis of rotating disks by setting all terms involving temperature equal to zero. The subject of design for prescribed centrifugal-stress distribution has likewise received only limited attention (examples of which may be found in references 6 and 7); the present method may therefore satisfy a need in this field of design.

DIRECT METHOD OF DISK DESIGN

Equations.—The equations for stress analysis of rotating disks are (reference 3)

$$\frac{d}{dr}(rh\sigma_r) - h\sigma_t + \rho\omega^2 hr^2 = 0 \qquad (1)$$

1

and

$$\frac{d}{dr}\left(\frac{\sigma_t}{E}\right)-\frac{d}{dr}\left(\frac{\mu\sigma_r}{E}\right)+\frac{d}{dr}(\alpha\Delta T)-\frac{(1+\mu)(\sigma_r-\sigma_t)}{Er}=0 \quad (2)$$

(All symbols are defined in the appendix.)

Equation (2) is a statement of the relation that must exist between the radial and tangential stress distributions, regardless of the shape of the disk, and therefore does not contain the disk thickness h. Once the stresses have been chosen to be compatible in accordance with equation (2), h can be determined from equation (1).

Solution of compatibility equation for specified stresses.— A finite-difference method for the solution of equations (1) and (2) is presented in reference 3. Choosing discrete point stations along a radius permits the stresses at the nth station to be expressed in terms of the stresses at the $(n\text{-}1)$st station. Equation (2) in finite-difference form becomes

$$C''_n\sigma_{r,n}-D'_n\sigma_{t,n}=F'_n\sigma_{r,n-1}-G'_n\sigma_{t,n-1}+H'_n \quad (3)$$

The coefficients C''_n, D'_n, and so forth are, in general, complicated expressions involving the radii r_n and r_{n-1} at the nth and $(n\text{-}1)$st stations as well as the properties of the disk material at the two stations. A great simplification in the expressions results if the radii r_n and r_{n-1} are not chosen at random, but are chosen according to a preselected schedule, for example, according to the relation

$$\frac{r_n-r_{n-1}}{r_n}=0.200$$

If, in addition, Poisson's ratio μ is assumed constant and equal to 0.333, equation (3) reduces to

$$1.133\,\sigma_{t,n}-0.466\,\sigma_{r,n}=\frac{E_n}{E_{n-1}}(0.833\,\sigma_{t,n-1}-0.166\,\sigma_{r,n-1})-E_nH'_n$$
$$=Z_n \quad (4)$$

Equation (4) is useful in the central region of the disk where values of r_n are relatively low. In order to obtain reasonable spacing of the point stations in the rim region where the radii are large, it is desirable to choose the spacing according to the relation

$$\frac{r_n-r_{n-1}}{r_n}=0.050$$

Equation (3) then becomes

$$1.033\sigma_{t,n}-0.366\sigma_{r,n}=\frac{E_n}{E_{n-1}}(0.965\sigma_{t,n-1}-0.298\sigma_{r,n-1})-$$
$$E_nH'_n=Z_n \quad (5)$$

As an example, equation (4) is considered. If $\sigma_{r,n-1}$ and $\sigma_{t,n-1}$ are already established and if the temperatures at the nth and $(n\text{-}1)$st station are known, the value of Z_n can be determined; then the only unknowns are $\sigma_{r,n}$ and $\sigma_{t,n}$. The equation is linear in $\sigma_{r,n}$ and $\sigma_{t,n}$ so that whatever are the actual values, a plot of $\sigma_{r,n}$ against $\sigma_{t,n}$ results in a straight line defined by equation (4). In order to establish the individual values of $\sigma_{r,n}$ and $\sigma_{t,n}$, another condition must be

specified. In some designs, specification of either the radial or the tangential stress may be desired; hence, the unspecified stress may then be directly determined from equation (4) or from the corresponding straight-line plot. A disadvantage of starting a design by specifying the radial or tangential stress is that the unspecified stress may be too high or in some other way unfavorable. It may be more desirable to specify the equivalent stress σ_e, which is defined by the equation

$$\sigma_{e,n}=\sqrt{\sigma_{r,n}^2-\sigma_{r,n}\sigma_{t,n}+\sigma_{t,n}^2} \quad (6)$$

This stress is usually used as the criterion for plastic-flow calculations (reference 4) and is therefore a logical design parameter. Furthermore, specification of the equivalent stress insures that neither the radial nor the tangential stress will be unexpectedly high. A plot of $\sigma_{r,n}$ against $\sigma_{t,n}$ for a given value of $\sigma_{e,n}$ results in an ellipse inclined at 45° to the coordinate axes. The intersection of the line defined by equation (4) and the ellipse of equation (6) defines the specific values of $\sigma_{r,n}$ and $\sigma_{t,n}$. Although, in general, a straight line intersects an ellipse at two points, the proper point for design use is usually obvious from the physical nature of the problem.

Design chart.— A design chart based on equations (4) and (6) is presented in figure 1(a). The straight lines correspond to different values of Z_n in equation (4) and the ellipses correspond to different values of equivalent stress $\sigma_{e,n}$. This chart is used to calculate the stresses at the nth station after the stresses have been determined at the $(n\text{-}1)$st station. The value of Z_n is calculated by equation (4) from conditions at the $(n\text{-}1)$st station and the temperature at the nth station, thereby establishing the line along which $\sigma_{r,n}$ and $\sigma_{t,n}$ must lie. Intersection of this line with the ellipse corresponding to the assigned value of equivalent stress at the nth station establishes $\sigma_{r,n}$ and $\sigma_{t,n}$. Thus, starting at a station near the center of the disk (or for a disk with a central hole, at the edge of the hole), where the radial and tangential stresses bear known relations to the equivalent stress, makes it possible to proceed with the determination of stresses at successive stations of increasing radius.

The corresponding chart for equation (5) is figure 1(b), which is used in determining the stress conditions in the rim region; whereas figure 1(a) is used for determining the stress conditions in the central region of the disk.

Determination of disk profile.— When the stresses have been determined, the shape of the disk can be obtained from the finite-difference equivalent of equation (1). For random values of r_n and r_{n-1}, the equation assumes the form

$$\frac{h_{n-1}}{h_n}=\frac{\left(\dfrac{2r_n}{r_n-r_{n-1}}\right)\sigma_{r,n}-\sigma_{t,n}+\rho_n\omega^2r_n^2}{\left(\dfrac{2r_{n-1}}{r_n-r_{n-1}}\right)\sigma_{r,n-1}+\sigma_{t,n-1}-\rho_{n-1}\omega^2r_{n-1}^2} \quad (7)$$

For $\dfrac{r_n-r_{n-1}}{r_n}=0.200$ and $\rho_n=\rho_{n-1}=$ constant density, equation (7) becomes

$$\frac{h_{n-1}}{h_n}=\frac{10.00\sigma_{r,n}-\sigma_{t,n}+\rho_nr_n^2\omega^2}{8.00\sigma_{r,n-1}+\sigma_{t,n-1}-0.640\rho_nr_n^2\omega^2} \quad (8)$$
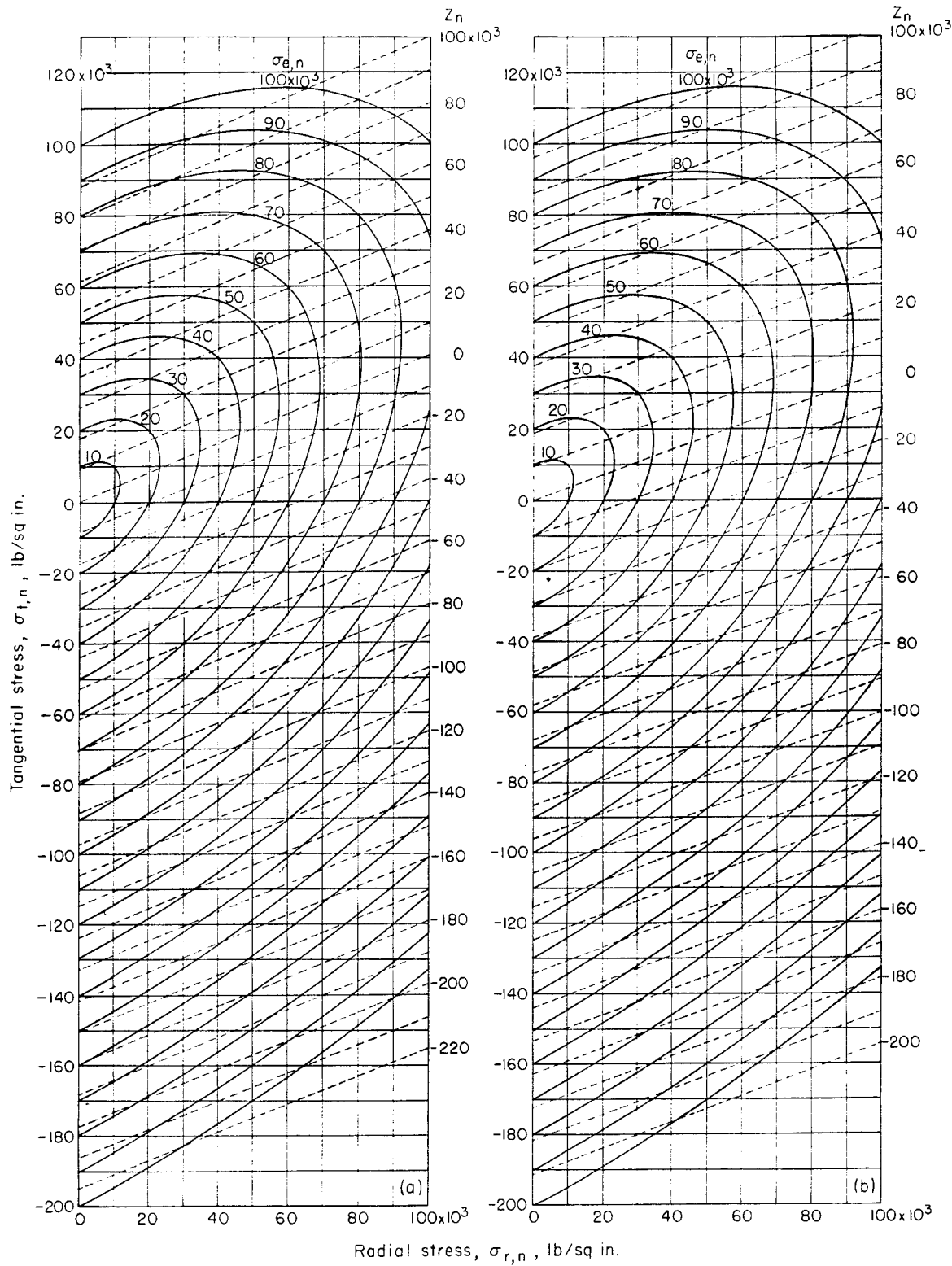
(a) $\frac{r_n - r_{n-1}}{r_n} = 0.200$.

(b) $\frac{r_n - r_{n-1}}{r_n} = 0.050$.

FIGURE 1.—Design charts for determining radial and tangential stresses.

and for $\dfrac{r_n - r_{n-1}}{r_n} = 0.050$ and $\rho_n = \rho_{n-1} =$ constant density, equation (7) becomes

$$\frac{h_{n-1}}{h_n} = \frac{40.00\sigma_{r,n} - \sigma_{t,n} + \rho_n r_n^2 \omega^2}{38.00\sigma_{r,n-1} + \sigma_{t,n-1} - 0.903\rho_n r_n^2 \omega^2} \tag{9}$$

Because equations (8) and (9) give only ratios of thickness and not specific thicknesses, a starting point for calculating actual thicknesses must be obtained from other considerations, for example, those at the rim. For disks with the familiar fir-tree blade attachments, one approach is as follows:

With reference to figure 2, if sufficient clearance is provided in the fastening between the blades and the disk to prevent circumferential tightening, the radial stress in the disk at the base of the serrations (at radius r_b) is the sum of the centrifugal stresses produced by the blades and by the serrated regions of the rim.

FIGURE 2.—Disk nomenclature for derivation of rim thickness.

The total centrifugal force due to airfoil sections of blades is

$$N\sigma_{bl}A_{bl} \tag{10}$$

The serrated bases of the blades and the base-retaining sections of the disk may be considered as a discontinuous ring of material subjected to centrifugal effect, the serrations serving to eliminate tangential stresses. When it is assumed that at the rim the thickness h_d (fig. 2) is specified from considerations of blade design and that the thickness tapers linearly to a value h_b (as yet to be determined) at the base of the serrated section of the disk, then approximately:
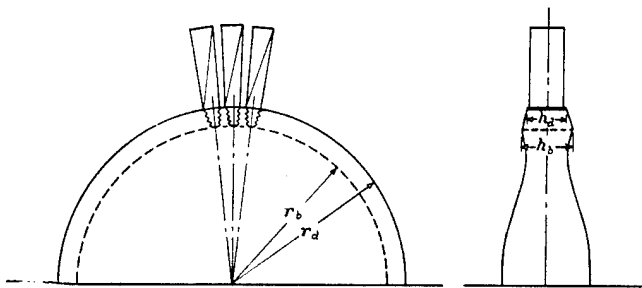
Total centrifugal force on serrated sections of blades and disk is

(speed²) (volume) (average density) (average radius)

or

$$\omega^2(r_d - r_b) \frac{(h_d + h_b)}{2} 2\pi \frac{(r_b + r_d)}{2} \rho \frac{(r_b + r_d)}{2} \tag{11}$$

The radial stress at the base of the slots is equal to the radial stress $\sigma_{r,b}$ at the rim of the continuous section of the disk and

presumably has already been determined from the disk design. Hence,

Total resisting force at rim of continuous disk

$$= \text{(stress) (area)}$$

$$= \sigma_{r,b} 2\pi r_b h_b \tag{12}$$

When the sum of equations (10) and (11) is equated to equation (12),

$$h_b = \frac{4N\sigma_{bl}A_{bl} + \pi\rho\omega^2(r_d + r_b)^2(r_d - r_b)h_d}{8\pi r_b \sigma_{r,b} - \pi\rho\omega^2(r_d + r_b)^2(r_d - r_b)} \tag{13}$$

When h_b has been determined, the thicknesses at the remaining stations in the disk may be obtained by successive multiplication by the ratio $\dfrac{h_{n-1}}{h_n}$. An application of the method is illustrated by the following example.

ILLUSTRATIVE DESIGN

Requirements.—The assumed problem is to design a disk of 9-inch radius to carry blades that require a 1.9-inch base thickness ($h_d = 1.9$). In order to retain the blades, a serrated region of 1-inch radial depth is necessary ($r_b = 9-1 = 8$ in.). Based on measurements of similar disks, the temperature distribution is assumed to be as shown in figure 3, and as an initial design, the equivalent stress at each location is assumed to be equal to the elastic limit of the material at the operating temperature. The disk is to operate at a speed of 11,850 rpm and the density of the disk and blade material is 0.29 pound per cubic inch.
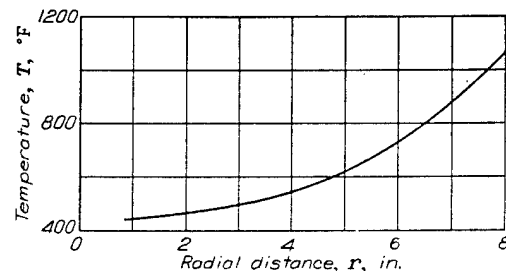
FIGURE 3.—Variation of temperature with disk radius assumed for illustrative design.

Establishment of stresses satisfying the compatibility equation.—The calculations are shown in table I. The disk is divided into 18 stations. Column 1 indicates the radius at each station as a fraction of the radius of the continuous section of the disk. These values have been chosen to yield nine stations with $\dfrac{r_n - r_{n-1}}{r_n} = 0.200$ and nine stations with $\dfrac{r_n - r_{n-1}}{r_n} = 0.050$. The actual value of r_n at each station is

obtained by multiplying the values of column 1 by the disk radius, which in this case is 8 inches. The radii are listed in column 2.

The difference between the actual temperature and the temperature at which there is no thermal stress is listed in column 3. Because in this case the stress-free condition is at a room temperature of 70° F, the ΔT_n term of column 3 is obtained by subtracting 70° F from the actual temperatures in figure 3.

The elastic moduli and the coefficients of thermal expansion at the operating temperatures of the various stations are listed in columns 4 and 5, respectively.

The values $\alpha_n \Delta T_n$, $H'_n = \alpha_n \Delta T_n - \alpha_{n-1} \Delta T_{n-1}$, and $E_n H'_n$ are then calculated as shown in columns 6, 7, and 8, respectively.

The quantity $r_n^2 \rho_n \omega^2$ at each station is then calculated, as shown in column 9. Column 10 lists values of the ratio $\dfrac{E_n}{E_{n-1}}$ needed for subsequent calculations.

Columns 11 and 12 are temporarily bypassed, and in column 13 the desired equivalent stress at each station is entered. In this design, the equivalent stresses are taken equal to the elastic limits of the material at the operating temperatures, which for the temperatures of figure 3 are shown in column 13.

The essential stress determinations are then effected by simultaneous operation on columns 11 to 15. At station a, the radial and tangential stresses are both equal to σ_e and are therefore both entered as 76,500 pounds per square inch in columns 14 and 15. These stresses are used to determine the value of Z at station 2 equal to 49,600, as listed in column 12. Reference to figure 1(a) then shows that the line $Z=49,600$ intersects the ellipse $\sigma_e=76,300$ at $\sigma_{r,n}=76,000$ and at $\sigma_{t,n}=75,000$, which are then listed in columns 14 and 15. In the same manner, these values are used to determine the stresses at station 3 and progressively at subsequent stations. For example, at station 8, $Z=32,200$ and $\sigma_e=75,000$. Intersection of the corresponding straight line and ellipse yields, in figure 1(a), $\sigma_{r,n}=83,000$ and $\sigma_{t,n}=62,000$.

At station 10, there is a change to $\dfrac{r_n-r_{n-1}}{r_n}=0.050$. The only effect is to change the coefficients in column 11 and to introduce the use of figure 1(b) instead of 1(a). At station 10, for example, $Z=13,800$ and $\sigma_e=73,000$. Intersection of the corresponding straight line and ellipse in figure 1(b) yields $\sigma_{r,n}=83,500$ and $\sigma_{t,n}=42,500$, which are listed in columns 14 and 15, and are subsequently used to obtain the value for Z at station 11. Thus, by successive and simultaneous operation on the various columns, values of $\sigma_{r,n}$ and $\sigma_{t,n}$ may be obtained for each station that are consistent with the compatibility equation and combine to yield

an equivalent stress at each station of any desired value. (If the imposed requirements are impossible to attain, the necessary straight line and ellipse will not intersect. Thus, for example, were it arbitrarily required to achieve an equivalent stress at the rim of 40,000 lb/sq in. while maintaining the equivalent stresses at all other stations at the values listed in column 13, the line $Z=60,900$ would not intersect the ellipse $\sigma_e=40,000$. The indication is merely that no physical disk can satisfy the requirements and that the requirements must be changed.)

Determination of disk profile.—Establishment of stresses by means of the compatibility equation makes it possible to obtain thickness ratios in accordance with equations (7) and (8). Before proceeding, however, examination of the radial stress at the rim $\sigma_{r,b}$ should be made in order to determine whether or not it will yield a reasonable value of thickness h_b in accordance with equation (13). Substitution of the values

$$N=54 \qquad C_{bi}=27,000$$

$$A_{bi}=0.625 \qquad \rho\omega^2=1150$$

$$r_b=8.00 \qquad r_d=9.00$$

$$h_d=1.9$$

in equation (13) results in the relation between h_b and $\sigma_{r,b}$ shown in figure 4. Obviously, from this figure, values of $\sigma_{r,b}$ below 18,000 pounds per square inch will yield inordinately large thickness values of h_b, whereas values of $\sigma_{r,b}$ above 40,000 pounds per square inch will yield inordinately low values while overstressing the rim material, which is operating at a high temperature. The allowable radial rim stress can be ascertained from a detailed analysis of creep strength and stress-rupture values of the rim material for the desired life of the wheel; but in any case, figure 4 indicates that the reasonable range for $\sigma_{r,b}$ is between 18,000 and 40,000 pounds per square inch.
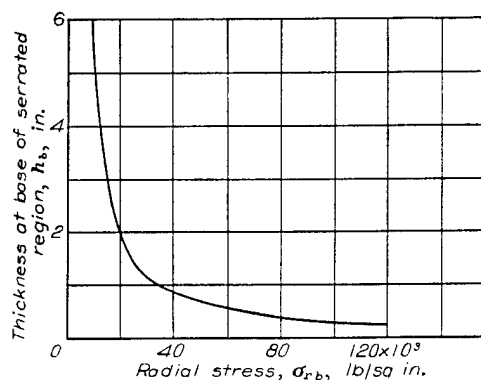

FIGURE 4.—Relation between thickness at rim of continuous section of disk and radial stress at that location.

Obviously, the value of $\sigma_{r,b}$ in table I obtained in the first determination ($\sigma_{r,b}$=approximately 0) does not lie within the aforementioned reasonable limits. The reason for the very low value of $\sigma_{r,b}$, however, is the designation of the low value of $\sigma_{t,b}$=58,000 pounds per square inch at rim of continuous section of disk. The compatibility condition demands only that $\sigma_{t,b}$ and $\sigma_{r,b}$ lie along the line $Z=60,900$ (column 12, table I). By modification of the demand on $\sigma_{t,b}$, the individual values of $\sigma_{t,b}$ and $\sigma_{r,b}$ can be moved to other locations along $Z=60,900$. Thus, for example, by a change in the requirements on $\sigma_{t,b}$ to 63,500, 64,000, 67,700, and 72,900 pounds per square inch, the values of $\sigma_{r,b}$ can be successively moved to 18,000, 20,000, 30,000, and 40,000 pounds per square inch with corresponding changes in $\sigma_{t,b}$; all these values are given in table I. Physically, the significance of this result is the impracticability of attempting to find a disk for which stresses at the rim will not exceed the elastic limit if all the other regions are to operate exactly at the elastic limit. Allowing the rim to operate somewhat above the elastic limit permits the remainder of the disk to be kept at the elastic limit. Under unusual conditions, modifying several stations near the rim may be necessary.

The values of $\dfrac{h_{n-1}}{h_n}$ are now computed according to equations (8) and (9), the necessary calculations being shown in columns 16, 17, and 18. Actual values of h_n are obtained in column 19 by successive multiplication by the ratio $\dfrac{h_{n-1}}{h_n}$ starting with the rim value h_b determined from figure 4 for each value of $\sigma_{r,b}$ and proceeding toward the center of the disk. The disk profiles and the stress distributions are shown in figure 5. The slenderness of the profiles relative to the rim is the result of operation at the elastic limit in most of the disk. More practical disks can be obtained by assuming σ_c values yielding greater factors of safety. The subject of allowable design stresses, however, requires considerable experimental investigation.
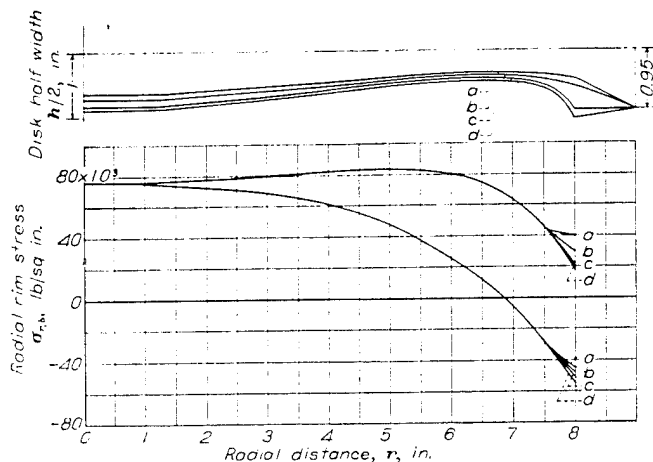
SIMPLIFIED METHOD OF STRESS ANALYSIS OF GIVEN DISK

ELASTIC STRESS

A method for calculating the elastic-stress distribution in a disk of given design is presented in reference 3. Although this method can be directly used to check the stress distribution in any disk designed by the procedure described herein, simplifications can be made that appreciably reduce the amount of labor involved in calculation.

Simplification of equations.—Briefly, the method of reference 3 consists in rewriting stress equations (1) and (2) in finite-difference form and solving these equations to obtain

$$\left.\begin{array}{l} \sigma_{r,n}=A_{r,n}\sigma_{t,a}+B_{r,n} \\ \sigma_{t,n}=A_{t,n}\sigma_{t,a}+B_{t,n} \end{array}\right\} \tag{14}$$

where $\sigma_{t,a}$ is the tangential stress at the first point station in the disk and remains unknown until the end of the calculation. The coefficients $A_{r,n}$ and so forth are determined from the equations

$$\left.\begin{array}{l} A_{r,n}=K_n A_{r,n-1}+L_n A_{t,n-1} \\ A_{t,n}=K'_n A_{r,n-1}+L'_n A_{t,n-1} \\ B_{r,n}=K_n B_{r,n-1}+L_n B_{t,n-1}+M_n \\ B_{t,n}=K'_n B_{r,n-1}+L'_n B_{t,n-1}+M'_n \end{array}\right\} \tag{15}$$

Thus, if the coefficients A_r, A_t, B_r, and B_t are known at the $(n-1)$st station, they are readily determined at the nth station from equations (15). The coefficients at the first station ($r=a$) are known. For a solid disk

$$\left.\begin{array}{l} A_{r,a}=A_{t,a}=1 \\ B_{r,a}=B_{t,a}=0 \end{array}\right\} \tag{16}$$

and for a disk with a central hole

$$\left.\begin{array}{l} A_{r,a}=B_{r,a}=B_{t,a}=0 \\ A_{t,a}=1 \end{array}\right\} \tag{17}$$

Hence, successive applications of equations (15) yield the coefficients for subsequent substitution in equations (14) for actual stress determinations. The value of $\sigma_{t,a}$ is determined from the condition at the rim where the radial stress is known. Thus, from the first of equations (14)

$$\sigma_{t,a}=\frac{\sigma_{r,b}-B_{r,b}}{A_{r,b}} \tag{18}$$

where $\sigma_{r,b}$ is the radial rim stress and $A_{r,b}$ and $B_{r,b}$ are the coefficients as determined in the last of the successive applications of equations (15).

The bulk of the computational work in a stress analysis is contained in the determination of the coefficients K_n, L_n, and so forth, in equations (15). When the stations are randomly chosen, the equations for these coefficients are complicated.

A great reduction in the amount of labor is effected if the stations are chosen according to an assigned value of $\frac{r_n - r_{n-1}}{r_n}$.

In addition, if Poisson's ratio is assumed constant as $\mu = 0.333$ the expressions assume the simplified form given in the following table:

TABLE A

	$\frac{r_n - r_{n-1}}{r_n} = 0.050$	$\frac{r_n - r_{n-1}}{r_n} = 0.200$
K_n	$0.959 \frac{h_{n-1}}{h_n} - 0.007 \frac{E_n}{E_{n-1}}$	$0.834 \frac{h_{n-1}}{h_n} - 0.015 \frac{E_n}{E_{n-1}}$
L_n	$0.025 \frac{h_{n-1}}{h_n} + 0.024 \frac{E_n}{E_{n-1}}$	$0.104 \frac{h_{n-1}}{h_n} + 0.077 \frac{E_n}{E_{n-1}}$
K'_n	$0.340 \frac{h_{n-1}}{h_n} - 0.291 \frac{E_n}{E_{n-1}}$	$0.343 \frac{h_{n-1}}{h_n} - 0.153 \frac{E_n}{E_{n-1}}$
L'_n	$0.009 \frac{h_{n-1}}{h_n} + 0.942 \frac{E_n}{E_{n-1}}$	$0.043 \frac{h_{n-1}}{h_n} + 0.767 \frac{E_n}{E_{n-1}}$
M_n	$-\left(0.023 \frac{h_{n-1}}{h_n} \rho_{n-1} + 0.025 \rho_n\right) r_n^2 \omega^2 - 0.024 E_n H'_n$	$-\left(0.067 \frac{h_{n-1}}{h_n} \rho_{n-1} + 0.104 \rho_n\right) r_n^2 \omega^2 - 0.092 E_n H'_n$
M'_n	$-\left(0.008 \frac{h_{n-1}}{h_n} \rho_{n-1} + 0.009 \rho_n\right) r_n^2 \omega^2 - 0.977 E_n H'_n$	$-\left(0.027 \frac{h_{n-1}}{h_n} \rho_{n-1} + 0.043 \rho_n\right) r_n^2 \omega^2 - 0.920 E_n H'_n$

Alinement charts.—Evaluation of the coefficients K_n, K'_n, and so forth from the expressions given in table A is possible. A further reduction in labor, however, can be effected by the use of the alinement charts in figure 6. For example, in figure 6(a), joining with a straight line the points $\frac{E_n}{E_{n-1}} = 0.987$ and $\frac{h_{n-1}}{h_n} = 1.185$ yields intersections on the suitable scales for values $L_n = 0.199$, $L'_n = 0.808$, $K_n = 0.972$, and $K'_n = 0.256$, which check closely with calculations based on the expressions in table A. If the density can be considered constant between two stations ($\rho_n = \rho_{n-1}$), the values of M_n and M'_n can also be obtained from the charts in figure 6. As an example, if $\frac{h_{n-1}}{h_n} = 1.185$, $r_n^2 \rho \omega^2 = 20.5 \times 10^3$, and $E_n H'_n = 5.5 \times 10^3$, the corresponding values of $\frac{h_{n-1}}{h_n}$ and $r_n^2 \rho \omega^2$ are joined by a straight line to determine the supplementary point P, which is then joined to $E_n H'_n = 5.5 \times 10^3$ to yield intersections $M_n = -4.3 \times 10^3$ and $M'_n = -6.6 \times 10^3$. Between any two stations where a change in density occurs, the expressions for M_n and M'_n in the table must be used.

Illustrative example.—The necessary calculations are shown in table II for the determination of the elastic stresses in a disk of given design, which are the disks formerly designed for the various assumed radial rim stresses. The coefficients K_n, L_n, and so forth listed in columns 20 to 25 are determined from values listed in table I used with the alinement charts of figure 6. Values beyond the range of the charts given in figure 6 may be computed from the equations given in table A. Columns 26 to 29 list the A and B coefficients as determined from equations (15) in which the

values listed in equations (16) are used as the initial conditions. The value of $\sigma_{t,a}$ is then determined with the aid of equation (18), and the radial and tangential stresses at all stations are obtained from equations (14) and listed in columns 30 and 31, respectively. The equivalent stresses at various stations are listed in column 32, and the yield stresses at each station, which were the design criterions, are listed in column 33. A correlation of satisfactory engineering accuracy exists between the computed stresses and the design stresses shown in columns 14 and 15 of table I.

PLASTIC STRESSES

Modification of elastic-stress equations.—A method for calculating the stress distribution in a disk subjected to plastic flow is presented in reference 4. The form of the calculation is similar to that of an elastic-stress determination, except that the term H'_n in the expression for M_n and M'_n (table A) is replaced by $H'_n - P'_n$, where P'_n depends on the plastic strains in the radial and tangential directions. In practice, the plastic strains are estimated and a stress distribution is determined. Comparison of the plastic strains based on the calculated stress values with the plastic strains assumed in order to determine these stresses permits better subsequent estimates. When resultant strain values agree closely with assumed strain values, the strains are assumed to be correct.

The values of P'_n to be used in the application of the simplified method are given in the following table:

TABLE B

$\frac{r_n - r_{n-1}}{r_n}$	P'_n
0.200	$0.100 \Delta_{r,n} + 0.125 \Delta_{r,n-1} - 1.100 \Delta_{t,n} + 0.875 \Delta_{t,n-1}$
0.050	$0.025 \Delta_{r,n} + 0.026 \Delta_{r,n-1} - 1.025 \Delta_{t,n} + 0.974 \Delta_{t,n-1}$

where $\Delta_{r,n}$ is the plastic radial strain at the nth station, and the other Δ terms represent other plastic strains according to the notation of this report. The detailed procedure for estimating the plastic strains and checking with computed values is given in reference 4.

Similarly for creep calculations, Q'_n terms are added to the P'_n terms, the form of the expressions being identical to those for P'_n in table B except that the Δ terms are replaced by creep terms δ, as discussed in reference 4.

Illustrative example.—As an illustration of practical procedure, the disk previously designed for a radial stress of 30,000 pounds per square inch at the rim is considered. As pointed out in the design calculations, any radial stress above 0 pounds per square inch at the rim will cause the equivalent stress to exceed the elastic limit; hence, plastic flow must occur. The amount of plastic flow in this case is small and is confined to the single station at the rim, but the method involved is essentially the same for the more complicated cases involving plastic flow at several stations and previously accumulated plastic flow and creep. Examination of reference 4 will indicate the procedure in the more complicated cases.

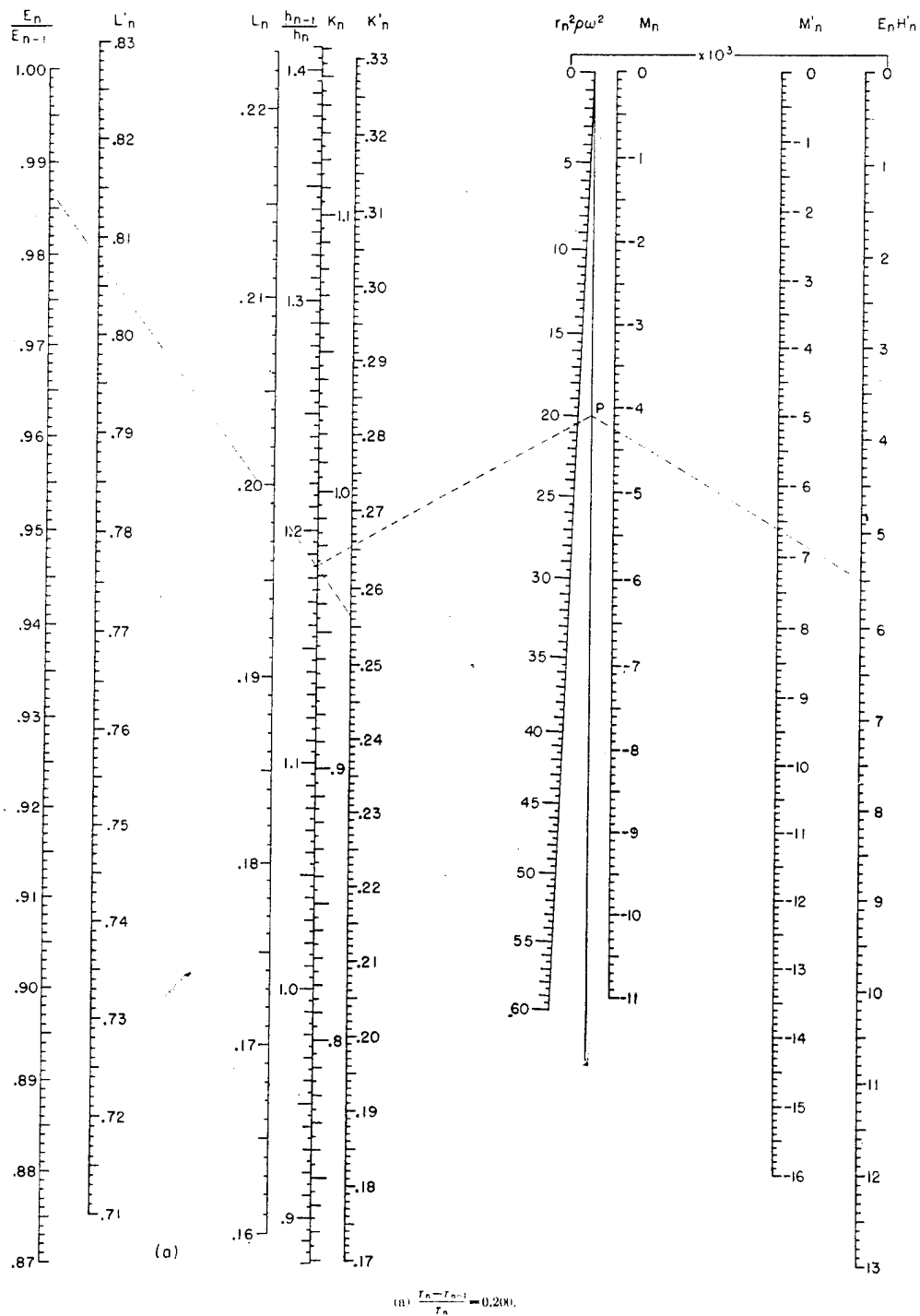(a) $\dfrac{r_n - r_{n-1}}{r_n} = 0.200.$

FIGURE 6.—Alinement charts for determining constants for finite-difference equations of stresses in turbine disks. $\rho_n = \rho_{n-1}$.
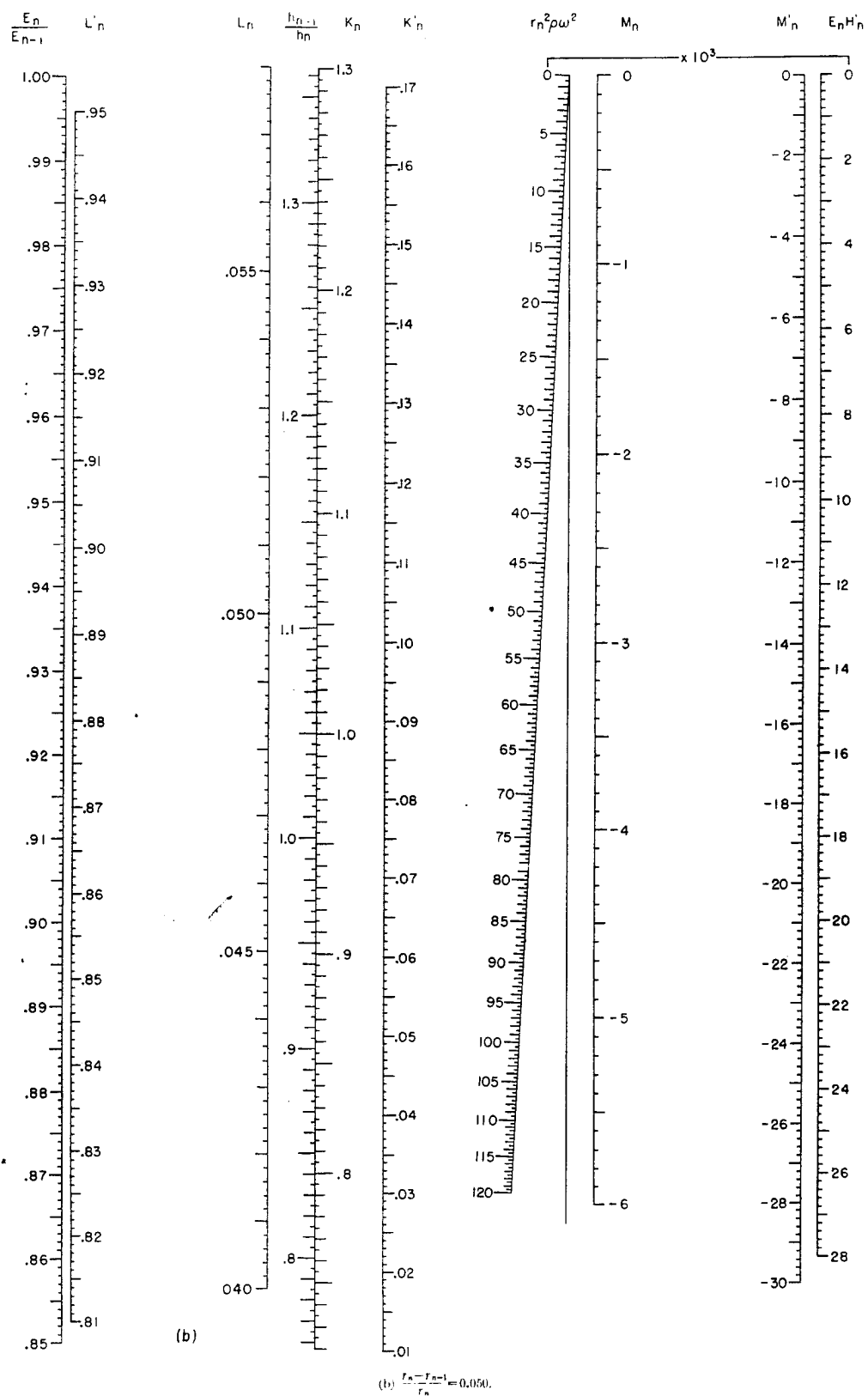
FIGURE 6.—Concluded. Alinement charts for determining constants for finite-difference equations of stresses in turbine disks. $r_n = r_{n-1}$.

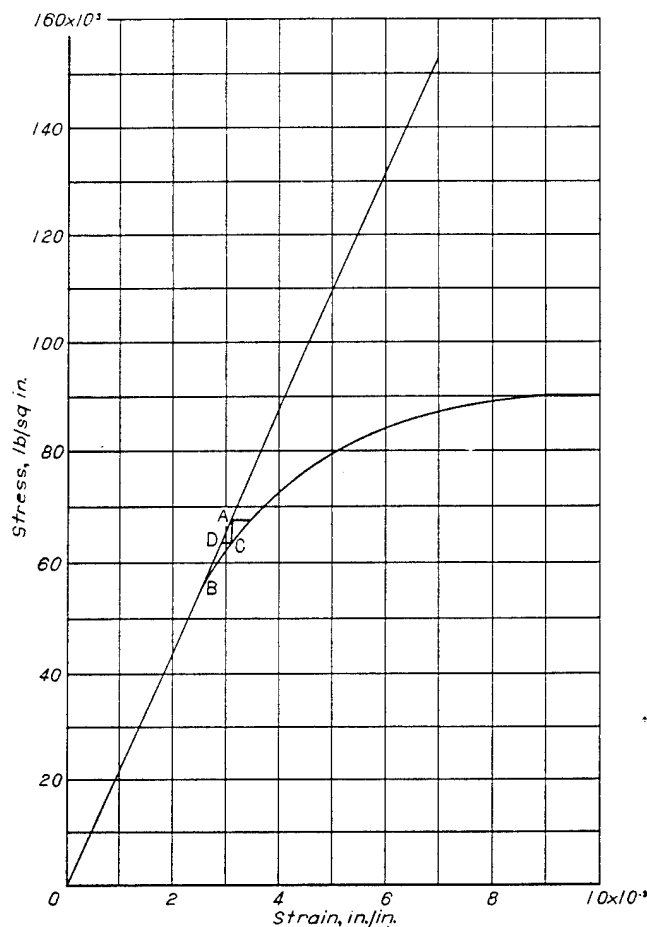(b) $\frac{r_n - r_{n-1}}{r_n} = 0.050.$

Figure 7.—Stress-strain curve for disk material at 1070° F.

COMMENT ON SIGNIFICANCE OF THERMAL STRESSES

The design method described assigns equal importance to the thermal and centrifugal stresses. The true relative importance of these two types of stress is, however, as yet to be evaluated. Whereas the centrifugal stresses are inherently necessary to balance the centrifugal forces of rotation—so that yielding due to overstressing in one region shifts the load and thereby increases the stress in another region—the thermal stresses constitute an internally balanced system. Tension in one region balances compression in others; hence, plastic flow in one region reduces the thermal stresses in another region. When considering bursting strength, for example, centrifugal stresses are probably of greater importance than thermal stresses. In the case of rim cracking (reference 8), which is in part due to cyclic plastic flow at the rim, the thermal stresses are, however, fully as important as the centrifugal stresses. Likewise, when disk deformations are considered in designing for close mechanical tolerances, thermal stresses must receive attention equal to that given to centrifugal stresses.

The relative importance of centrifugal and thermal stresses depends, to a great extent, on the ductility of the disk material. As yet, experimental data are very meager on the significance of ductility. In any case, however, because the distinction between the two types of stress can only be realized after the occurrence of plastic flow and because the behavior of a material in subsequent loading depends on its previous stress-strain history, thermal stresses should receive detailed attention early in the design in order to minimize any detrimental effects that may result from their omission.

The stress-strain curve for the disk material at the operating temperature of 1070° F is given in figure 7. Point A is the calculated elastic equivalent stress at the rim, B the yield point, and C the intersection with the stress-strain curve of a vertical line drawn through A. In accordance with the method of reference 4, the strain CD is the first approximation of the plastic strain. The value is listed in columns 34 and 35 of table III for station b. Columns 36 and 37 list the approximated radial and tangential plastic strains obtained from equations (20) of reference 4. The value of P'_n as determined from table B, is listed in column 38. Column 39 corresponds to column 8 of table I used in the elastic-stress calculations; the only difference is that $II'_n - P'_n$ has replaced II_n. From this point, the calculations are identical to elastic-stress calculations and are shown in columns 24, 25, and 28 to 32 (table III), which are similar to the corresponding columns of table II. Further approximations, made in accordance with the method of reference 4, are also shown in table III to obtain greater accuracy of approximation.

REFERENCES

1. Stodola, A.: Steam and Gas Turbines, vol. 1. McGraw-Hill Book Co., Inc., 1927. (Reprinted, Peter Smith (New York), 1945.)
2. Thompson, A. Stanley: Stresses in Rotating Disks at High Temperatures. Jour. Appl. Mech., vol. 13, no. 1, March 1946, pp. A45–A52.
3. Manson, S. S.: Determination of Elastic Stresses in Gas-Turbine Disks. NACA Rep. 871, 1947.
4. Millenson, M. B., and Manson, S. S.: Determination of Stresses in Gas-Turbine Disks Subjected to Plastic Flow and Creep. NACA Rep. 906, 1948.
5. Leopold, W. R.: Centrifugal and Thermal Stresses in Rotating Disks. Jour. Appl. Mech., vol. 15, no. 4, Dec. 1948, pp. 322–326.
6. McDowell, C. M.: Prescribed-Centrifugal-Stress Design of Rotating Discs. Paper presented before SAE Ann. Meeting (Detroit), Jan. 12–16, 1948.
7. Tumarkin, S.: Methods of Stress Calculation in Rotating Disks. NACA TM 1064, 1944.
8. Manson, S. S.: Stress Investigations in Gas Turbine Discs and Blades. SAE Quarterly Trans., vol. 3, no. 2, April 1949, pp. 229–239.

APPENDIX

SYMBOLS

In addition to the symbols used herein, the symbols of references 3 and 4 of which application is made in this report are defined. The various coefficients are given in their general form for random spacing of the point stations. From these coefficients, the simplified coefficients can be obtained by direct substitution of $\frac{r_n - r_{n-1}}{r_n} = $ constant and $\mu = $ constant.

A_{bl}	base area of airfoil section of blade, sq in.
E	elastic modulus of disk material, lb/sq in.
h	axial thickness of disk, in.
N	number of blades supported by disk
r	radial distance, in.
T	temperature, °F
α	coefficient of thermal expansion between actual temperature and temperature at zero thermal stress, in./(in.)(°F)
Δ	plastic increment of strain, in./in.
Δ_r	plastic increment of strain in radial direction, in./in.
Δ_t	plastic increment of strain in tangential direction, in./in.
ΔT	temperature increment above temperature of zero thermal stress, °F
δ_r	creep increment in radial direction, in./in.
δ_t	creep increment in tangential direction, in./in.
ϵ_p	plastic strain corresponding to stress σ_e in tensile specimen, in./in.
μ	Poisson's ratio
ρ	mass density of disk material, (lb) (sec²)/in.⁴
σ_{bl}	stress at base of airfoil section of blade, lb/sq in.
σ_e	equivalent stress, lb/sq in.
σ_r	radial stress, lb/sq in.
σ_t	tangential stress, lb/sq in.
σ_y	proportional elastic limit, lb/sq in.
ω	angular velocity, radians/sec

The following supplementary subscripts are used for denoting values of the preceeding symbols in connection with the finite-difference solution:

n	nth point station
$n-1$	$(n-1)$st point station
a	station at smallest disk radius considered (For disk with a central hole, this station is taken at the radius of the central hole; for a solid disk, this station is taken at a radius approximately 10 percent of the rim radius, which is larger than that (5 percent) recommended in reference 3. The value of 10 percent yields results of satisfactory accuracy and permits the use of fewer stations when constant value of $\frac{r_n - r_{n-1}}{r_n}$ is used.)
b	station at rim of continuous section of disk or base of blades
d	station at rim of disk or base of airfoil section of blades

The following supplementary symbols denote combinations of the previous symbols:

$$\left.\begin{array}{l} A_{r,n} \\ A_{t,n} \\ B_{r,n} \\ B_{t,n} \end{array}\right\} \begin{array}{l} \text{stress coefficients defined by equations} \\ \sigma_{r,n} = A_{r,n}\sigma_{t,a} + B_{r,n} \\ \sigma_{t,n} = A_{t,n}\sigma_{t,a} + B_{t,n} \end{array}$$

$$C_n = r_n h_n$$

$$C'_n = \frac{\mu_n}{E_n} + \frac{(1+\mu_n)(r_n - r_{n-1})}{2E_n r_n}$$

$$D_n = \frac{1}{2}(r_n - r_{n-1})h_n$$

$$D'_n = \frac{1}{E_n} + \frac{(1+\mu_n)(r_n - r_{n-1})}{2E_n r_n}$$

$$F_n = r_{n-1}h_{n-1}$$

$$F'_n = \frac{\mu_{n-1}}{E_{n-1}} - \frac{(1+\mu_{n-1})(r_n - r_{n-1})}{2E_{n-1}r_{n-1}}$$

$$G_n = \frac{1}{2}(r_n - r_{n-1})h_{n-1}$$

$$G'_n = \frac{1}{E_{n-1}} - \frac{(1+\mu_{n-1})(r_n - r_{n-1})}{2E_{n-1}r_{n-1}}$$

$$H_n = \frac{1}{2}\omega^2(r_n - r_{n-1})(\rho_n h_n r_n^2 + \rho_{n-1}h_{n-1}r_{n-1}^2)$$

$$H'_n = \alpha_n \Delta T_n - \alpha_{n-1}\Delta T_{n-1}$$

$$K_n = \frac{F'_n D_n - F_n D'_n}{C'_n D_n - C_n D'_n}$$

$$K'_n = \frac{C_n F'_n - C'_n F_n}{C'_n D_n - C_n D'_n}$$

$$L_n = -\frac{G'_n D_n + G_n D'_n}{C'_n D_n - C_n D'_n}$$

$$L'_n = -\frac{C'_n G_n + C_n G'_n}{C'_n D_n - C_n D'_n}$$

$$M_n = \frac{D'_n H_n + D_n(H'_n - P'_n - Q'_n)}{C'_n D_n - C_n D'_n}$$

$$M'_n = \frac{C'_n H_n + C_n(H'_n - P'_n - Q'_n)}{C'_n D_n - C_n D'_n}$$

(M_n and M'_n are defined in the elastic case for $P''_n = Q'_n = 0$)

$$P'_n = \Delta_{r,n}\left(\frac{r_n - r_{n-1}}{2r_n}\right) + \Delta_{r,n-1}\left(\frac{r_n - r_{n-1}}{2r_{n-1}}\right) -$$

$$\Delta_{t,n}\left(1 + \frac{r_n - r_{n-1}}{2r_n}\right) + \Delta_{t,n-1}\left(1 - \frac{r_n - r_{n-1}}{2r_{n-1}}\right)$$

$$Q'_n = \delta_{r,n}\left(\frac{r_n - r_{n-1}}{2r_n}\right) + \delta_{r,n-1}\left(\frac{r_n - r_{n-1}}{2r_{n-1}}\right) -$$

$$\delta_{t,n}\left(1 + \frac{r_n - r_{n-1}}{2r_n}\right) + \delta_{t,n-1}\left(1 - \frac{r_n - r_{n-1}}{2r_{n-1}}\right)$$

For $\frac{r_n - r_{n-1}}{r_n} = 0.050$,

$$Z_n = \frac{E_n}{E_{n-1}}(0.965\sigma_{t,n-1} - 0.298\sigma_{r,n-1}) - E_n H'_n$$

For $\frac{r_n - r_{n-1}}{r_n} = 0.200$,

$$Z_n = \frac{E_n}{E_{n-1}}(0.833\sigma_{t,n-1} - 0.166\sigma_{r,n-1}) - E_n H'_n$$

TABLE I.—CALCULATION OF DISK PROFILES FOR ILLUSTRATIVE DESIGN

n	$\dfrac{r_n-r_{n-1}}{r_n}$	1 $\dfrac{r_n}{r_b}$	2 $r_n,$ $r_b\times(1)$	3 ΔT_n	4 E_n	5 α_n	6 $\alpha_n\Delta T_n$ $(3)\times(5)$	7 H'_n $(6)-(6)_{n-1}$	8 $E_n H'_n$ $(4)\times(7)$	9 $r_n^2\rho_n\omega^2,$ $(2)^2\times1150$	10 $\dfrac{E_n}{E_{n-1}}$ $(4)\div(4)_{n-1}$
a	0.200	0.106	0.848	370	28.6×10^6	8.89×10^{-6}	3.289×10^{-3}	0.049×10^{-3}	1.40×10^3	1.28×10^3	1.000
2	.200	.132	1.056	375	28.6	8.90	3.338	.044	1.25	2.00	.997
3	.200	.165	1.320	380	28.5	8.90	3.382	.048	1.37	3.12	1.000
4	.200	.206	1.648	385	28.5	8.91	3.430	.097	2.75	4.90	.996
5	.200	.258	2.064	395	28.4	8.93	3.527	.143	4.05	7.63	.996
6	.200	.322	2.576	410	28.3	8.95	3.670	.245	6.91	11.95	.996
7	.200	.403	3.224	435	28.2	9.00	3.915	.339	9.49	18.70	.993
8	.200	.504	4.032	470	28.0	9.05	4.254	.898	24.61	29.19	.979
9	.200	.630	5.040	560	27.4	9.20	5.152	.201	5.49	32.35	.996
10	.050	.663	5.304	580	27.3	9.23	5.353	.308	8.32	35.86	.989
11	.050	.698	5.584	610	27.0	9.28	5.661	.357	9.57	39.76	.993
12	.050	.735	5.880	645	26.8	9.33	6.018	.421	11.16	43.98	.989
13	.050	.773	6.184	685	26.5	9.40	6.439	.481	12.55	48.77	.985
14	.050	.814	6.512	730	26.1	9.48	6.920	.585	14.98	54.05	.981
15	.050	.857	6.856	785	25.6	9.56	7.505	.658	16.32	59.88	.969
16	.050	.902	7.216	845	24.8	9.66	8.163	.728	17.11	66.42	.948
17	.050	.950	7.600	910	23.5	9.77	8.891	1.029	22.02	73.60	.911
b	.050	1.000	8.000	1000	21.4	9.92	9.920				

n	11 $0.833\times(15)_{n-1}$ $-0.166\times(14)_{n-1}$	12 $Z_n,$ $(11)\times(10)-(8)$	13 $\sigma_{\theta,n}$	14 $\sigma_{r,n}$	15 $\sigma_{t,n}$	16 $8.00\times(14)_{n-1}+$ $(15)_{n-1}-0.64\times(9)$	17 $10.00\times(14)$ $-(15)+(9)$	18 $\dfrac{h_{n-1}}{h_n},$ $(17)\div(16)$	19 $h_n,(18)_{n+1}\times(19)_{n+1}$ $\sigma_{r,b}=18{,}000$	19 $\sigma_{r,b}=20{,}000$	19 $\sigma_{r,b}=30{,}000$	19 $\sigma_{r,b}=40{,}000$
a			76.5×10^3	76.5×10^3	76.5×10^3	688×10^3 *	686×10^3	0.997	1.86	1.75	1.50	1.36
2	51.0×10^3	49.6×10^3	76.3	76.0	75.0	682	688	1.009	1.87	1.76	1.50	1.36
3	49.9	48.5	76.2	76.0	74.0	680	700	1.029	1.85	1.74	1.49	1.35
4	49.0	47.6	76.1	77.0	73.0	686	713	1.039	1.80	1.69	1.45	1.31
5	48.0	45.1	76.0	78.0	72.0	691	727	1.052	1.73	1.63	1.40	1.26
6	47.0	42.8	75.9	79.0	70.5	695	750	1.079	1.64	1.55	1.33	1.20
7	45.6	38.5	75.5	80.5	66.5	699	787	1.126	1.52	1.44	1.23	1.11
8	42.0	32.2	75.0	83.0	62.0	707	823	1.164	1.35	1.28	1.09	.99
9	37.9	12.5	73.5	84.0	46.0				1.16	1.10	.94	.85
	$0.965\times(15)_{n-1}$ $-0.298\times(14)_{n-1}$					$38.00\times(14)_{n-1}+$ $(15)_{n-1}-0.903\times(9)$	$40.00\times(14)$ $-(15)+(9)$					
10	19.4×10^3	13.8	73.0	83.5	42.5	3209×10^3	3330×10^3	1.038	1.12	1.06	.91	.82
11	16.1	7.6	72.5	83.0	36.5	3183	3319	1.043	1.07	1.02	.87	.79
12	10.5	.8	71.5	82.0	29.5	3155	3290	1.043	1.03	.98	.83	.76
13	4.0	−7.2	70.5	78.5	21.0	3106	3163	1.018	1.01	.96	.82	.75
14	−3.1	−15.6	69.5	74.5	11.5	2960	3017	1.019	.99	.94	.80	.74
15	−11.1	−25.9	68.0	67.0	−1.0	2794	2735	.979	1.01	.96	.82	.76
16	−20.9	−36.6	65.8	56.5	−16.0	2491	2336	.938	1.08	1.02	.87	.81
17	−32.3	−47.7	63.0	43.0	−31.0	2071	1817	.877	1.23	1.16	.99	.92
b	−42.7	−60.9	60.0	0	−60.0	1537	134	.087	2.23	------	------	------
b	−42.7	−60.9	63.5	18.0	−53.0	1537	847	.551	------	1.93	------	------
b	−42.7	−60.9	64.0	20.0	−52.0	1537	926	.602	------	------	1.15	------
b	−42.7	−60.9	67.7	30.0	−48.0	1537	1322	.860	------	------	------	------
b	−42.7	−60.9	72.9	40.0	−44.5	1537	1718	1.118	------	------	------	.82

TABLE II.—CALCULATION OF ELASTIC STRESSES FOR ILLUSTRATIVE DESIGN

	20	21	22	23	24	25	26	27	28	29	30	31	32	33
	K_n	L_n	K'_n	L'_n	M_n	M'_n	$A_{r,n}$	$A_{t,n}$	$B_{r,n}$	$B_{t,n}$	$\sigma_{r,n}$	$\sigma_{t,n}$	$\sigma_{e,n}$	$\sigma_{y,n}$
n		From table I, (18) and (16)				(18), (9), (8)	$(20)\times(26)_{n-1}$ $+(21)\times(27)_{n-1}$	$(22)\times(26)_{n-1}$ $+(23)\times(27)_{n-1}$	$(20)\times(28)_{n-1}$ $+(21)\times(29)_{n-1}$ $+(24)$	$(22)\times(28)_{n-1}$ $+(23)\times(29)_{n-1}$ $+(25)$	$\sigma_{r,a}=\frac{(\sigma_{r,b}-B_{r,b})}{A_{r,b}}=76,100$		$\sqrt{(30)^2+(31)^2}$ $-(30)\times(31)$	
		Coefficients determined from figure 6 or from table A									$\sigma_{r,a}\times(26)$ $+(28)$	$\sigma_{r,a}\times(27)$ $+(29)$		
a	0.816	0.180	0.189	0.810	-0.4×10^3	-1.4×10^3	1.000	1.000	0	0	76.1×10^3	76.1×10^3	76.1×10^3	76.5×10^3
2	.826	.181	.194	.808	$-.5$	-1.3	.996	.999	-0.4×10^3	-1.4×10^3	75.4	74.6	75.0	76.3
3	.843	.184	.200	.811	$-.7$	-1.5	1.004	1.000	-1.1	-2.5	75.3	73.6	74.5	76.2
4	.851	.184	.204	.809	-1.1	-2.9	1.030	1.012	-2.1	-3.7	76.3	73.3	74.8	76.1
5	.862	.186	.208	.809	-1.7	-4.3	1.063	1.028	-3.6	-6.3	77.3	71.9	74.7	76.0
6	.885	.189	.218	.810	-2.7	-7.2	1.108	1.053	-6.0	-10.1	78.3	70.0	74.5	75.9
7	.924	.193	.234	.810	-4.2	-10.1	1.180	1.094	-9.9	-16.7	79.9	66.6	74.1	75.5
8	.956	.196	.249	.801	-7.6	-24.8	1.301	1.162	-16.6	-25.9	82.4	62.5	74.5	75.0
9	.988	.050	.063	.947	-1.7	-5.9	1.472	1.255	-28.5	-49.7	83.5	45.8	72.4	73.5
10	.993	.050	.067	.941	-2.0	-8.8	1.517	1.281	-32.3	-54.8	83.1	42.7	72.0	73.0
11	.993	.050	.066	.945	-2.2	-10.0	1.570	1.307	-36.8	-62.5	82.7	37.0	71.8	72.5
12	.969	.049	.058	.941	-2.4	-11.7	1.624	1.339	-41.9	-71.5	81.7	30.4	71.5	71.5
13	.970	.049	.060	.937	-2.7	-13.1	1.639	1.354	-46.5	-81.4	78.2	21.6	69.9	70.5
14	.932	.048	.047	.933	-2.9	-15.5	1.656	1.367	-51.8	-92.2	74.2	11.8	69.1	69.5
15	.892	.047	.037	.921	-3.2	-16.9	1.609	1.353	-55.6	-104.0	66.8	-1.0	67.3	68.0
16	.834	.044	.022	.901	-3.4	-17.8	1.499	1.306	-57.7	-114.7	56.4	-15.3	65.4	65.8
17							1.303	1.210	-56.6	-122.4	42.9	-30.3	63.7	63.0
b	.522	.035	$-.078$	.863	-3.3	-22.4	.725	.942	-37.1	-123.6	18.0	-51.9	62.9	58.0
b	.571	.037	$-.060$	.864	-3.4	-22.5	.792	.967	-40.2	-124.9	20.0	-51.3	63.8	58.0
b	.818	.043	.027	.866	-3.9	-22.7	1.122	1.083	-55.5	-130.2	30.0	-47.8	67.9	58.0
b	1.066	.050	.115	.868	-4.3	-22.9	1.455	1.201	-70.8	-135.7	40.0	-44.3	73.0	58.0

TABLE III.—CALCULATION OF PLASTIC STRESSES FOR ILLUSTRATIVE DESIGN

$[\sigma_{r,b}=30,000]$

						$\dfrac{r_n-r_{n-1}}{r_n}$										
						0.200	0.050									
		34	35	36	37	38	38	39	24	25	28	29	30	31	32
n	Approximation	$\epsilon_{p,n}$	$\epsilon_{p,n}$	$\Delta_{r,n}$	$\Delta_{t,n}$	P'_{n}	P'_{n}	$E_n(H'_n-P'_n)$	M_n	M'_n	$B_{r,n}$	$B_{t,n}$	$\sigma_{r,n}$	$\sigma_{t,n}$	$\sigma_{e,n}$
		(fig. 7)	(estimate)	$\dfrac{0.50\times(35)}{(32)}\times$ $[2\times(30)-(31)]$	$\dfrac{0.50\times(35)}{(32)}\times$ $[2\times(31)-(30)]$	$0.100(36)+$ $0.125(36)_{n-1}$ $-1.100(37)+$ $0.875(37)_{n-1}$	$0.025(36)+$ $0.026(36)_{n-1}$ $-1.025(37)+$ $0.974(37)_{n-1}$	$(4)\times$ $[(7)-(38)]$	From fig. 6 using cols. (9), (18), and (39)		$(20)\times(28)_{n-1}$ $+(21)\times(29)_{n-1}$ $+(24)$	$(22)\times(28)_{n-1}$ $+(23)\times(29)_{n-1}$ $+(25)$	$\sigma_{r,a}\times(26)$ $+(28)$	$\sigma_{t,a}\times(27)$ $+(29)$	$\sqrt{(30)^2+(31)^2}$ $-(30)\times(31)$
17	1	0	0	0	0		0.194×10^3	17.9×10^3	-3.7×10^3	-18.7×10^3		-55.3×10^3	-126.2×10^3	30.0×10^3	-43.9×10^3	64.4×10^3
b		$.20\times10^3$	$.20\times10^3$	$.159\times10^3$	$-.185\times10^3$											
17	2	0	0	0	0		$.201$	17.7	-3.7	-18.5		-55.3	-126.0	30.0	-43.7	64.2
b		.22	.21	.169	$-.192$											